FINAL REPORT

NAS 8--31731

"VAPOR TRANSPORT MECHANISMS"

Prepared For:

George C. Marshall Space Flight Center

Marshall Space Flight Center, Alabama 35812

August 7, 1978

Principal Investigator:

Dr. Gary L. Workman

Athens State College

Athens, Alabama 35611

FINAL REPORT

NAS 8-31731

"Vapor Transport Mechanisms"

Prepared for:

George C. Marshall Space Flight Center

Marshall Space Flight Center, Alabama 35812

August 7, 1978

Principal Investigator:

Dr. Gary L. Workman

Athens State College

Athens, AL 35611

ABSTRACT

The Raman scactering furnace for investigating vapor transport mechanisms has been completed and checked out. Preliminary experiments demonstrate that a temperature resolution of $\pm 5°C$ is possible with this system operating in a backscatter mode. In the experiments presented here with the GeI_4 plus excess Ge system at temperatures up to 600°C, only the GeI_4 band at 150 cm^{-1} has been observed. Further experiments are in progress to determine if GeI_2 does become the major vapor species above 440°C.

TABLE OF CONTENTS

INTRODUCTION

The use of chemical vapor transport for the growth of single crystalline materials has increased considerably in recent years. A number of materials of varying degrees of complexity, such as Gd_4GeS_6 or GeSe[1], have been grown using chemical vapor transport techniques. The determination of the proper experimental conditions for good crystal growth is performed primarily by trial and error, even today. A significant portion of the research carried out in chemical vapor transport experiments is primarily concerned with developing a basic understanding of the critical parameters in the chemical vapor transport of single crystal materials.

A large part of the driving force for studying vapor transport mechanisms has been due to high purity electronic materials grown using this technique and also due to some interesting results from chemical vapor transport experiments performed in a microgravity environment on Skylab and ASTP Orbital Space Flights by Weidemeier.[2,3,4] These flight experiments studied the vapor transport of several combinations of germanium compounds (GeSe, GeTe, GeS) using either germanium tetraiodide or germanium tetrachloride for the transport agent. In all cases the transport rates were significantly greater than predicted from either experimentally extrapolated data or from the calculations of Weidemeier using several generally accepted methods based on models proposed by Schafer[5], Lever[6],

Mandel[7], and Faktor[7]. The crystalline quality of the crystals grown in the microgravity environment was superior to those grown on the ground using the same methods, even with the higher than expected transport rates. Since no satisfactory explanation exists for the increased microgravity transport, it is generally felt that we still need to know more about the basic fundamentals of chemical vapor transport phenomena. In order to contribute some information about the chemistry involved in such experiments we have attempted to determine more accurately the gaseous compositions and temperature of chemical vapor transport systems using laser Raman spectroscopic techniques. This report is concerned primarily with the results obtained with GeI_4-Ge system, particularly in the temperature measurements, using laser Raman techniques.

BACKGROUND

The literature contains a number of experimental studies dealing with the germanium iodine system. The treatise by Rolston[9] presents an excellent background on the chemistry of the system, as well as the inconsistencies in some observations of the complex equilibria occurring at high temperatures. The most consistent data which indicated that the important disproportionation reaction

(1) $GeI_4(v) + Ge(s) = 2\ GeI_2(v)$

would shift directions around 440°C was presented by Lever.[10] The thermodynamic analysis of Lever's work also allowed him to determine the equilibrium constants of reaction (1) above as well as for:

(2) $GeI_4(v) = GeI_2(v) + I_2(v)$

It was determined that reaction (1) should be the dominating process in the chemical vapor transport of germanium vi. the iodides. The thermodynamic data of Lever's has been the most widely accepted data. More consideration of this data is presented in a later section where our calculations also predicted reaction (1) to be the most predominant process at higher temperatures.

In its most obvious sense reaction (1) indicates that $GeI_4(v)$ can take up Ge(s) and transport the germanium as GeI_2, and then deposit Ge at the cooler end of the temperature gradient. The simplicity of the process should enable reaction (1) to be demonstrated either experimentally or theoretically to predict

the observed data in micro-gravity. Unfortunately it does not.

The analytical techniques which were considered for the experimental identification of the equilibrium composition included mass spectrometry, optical absorption, infra-red absorption, and laser Raman spectroscopy. Laser Raman spectroscopy was chosen, since it was the only technique which could be used with the particular type of furnace used in this work. Several advantages of laser Raman spectroscopy are that the signal is proportional to the concentration, the frequency shift can be used to identify the molecular species, and that the temperature of the gas can be determined internally.

The theory of Raman Spectroscopy and its many applications has been treated by many authors.[11-15] For now we are primarily concerned with two functional relationships dealing with Raman scattering intensities versus concentration and temperature. For a definition of the terms used throughout this report we refer to Figure 1. When monochromatic radiation of frequency ν_e passes through a nonabsorbing medium, the scattered light which emanates from the excitation region can posses new frequencies depending upon the gas composition. Dr. C.V. Raman demonstrated this effect in 1928 and since that time the process is identified as Raman scattering or Raman spectroscopy. As seen in Figure 1, the scattered frequencies can be described by their frequency shifts from ν_e. For instance, this example illustrates the observed frequencies $(\nu_e - \Delta\nu_b)$, $(\nu_e - \Delta\nu_a)$, ν_e, $(\nu_e - \Delta\nu_a)$, and $(\nu_e + \Delta\nu_b)$; listed in order of increasing frequency

or decreasing wavelength. The observed frequencies smaller than ν_e are called Stokes scattering while the observed frequencies larger than ν_e are called anti-Stokes scattering. The scattered radiation having frequency ν_e (unshifted) is called Rayleigh scattering and represents the largest portion of the scattered radiation by a factor of about 10^6.

The functional relationship used to derive intensity and compositional relationships is given by:

$$(3) \quad I_i = K (\nu_E \pm \Delta\nu_i)^4 I_E \rho \sigma_{i,T}$$

where
- K - Constant whose value depends upon experimental optics
- ν_e - laser excitation frequency
- $\Delta\nu_i$ - Raman frequency shift for component i
- I_E - excitation laser intensity
- ρ - Number density of molecular species i
- $\sigma_{i,T}$ - Raman scattering cross-section for species i at temperature T

The Raman data obtained with the GeI_4-Ge samples will thus provide the following information. From the frequency shift of the observed Raman signal, the identity of the scattering molecule can be deduced. Upon taking the ratio of the anti-Stoke signal to the Stokes signal, the temperature can be obtained with the following relation:

$$(4) \quad R = \frac{I (\nu_E - \Delta\nu_i)}{I (\nu_E + \Delta\nu_i)} = \frac{(\nu_E + \Delta\nu_i)^4}{(\nu_E + \Delta\nu_i)^4} \exp\left(-\frac{h\Delta\nu_i}{kT}\right)$$

The accuracy of the anti-Stokes/Stokes method is improved when integrated peak areas are used, rather than just peak blights. Since the Raman signals are usually quite weak compared to certain argon emission lines which occur in the same spectral regions as the desired Raman bands, integrated areas should represent a more accurate definition of the peak profile also.

The thermodynamics of chemical vapor transport reactions can be very complicated when all equilibria are taken into consideration. For example, a temperature dependent process such as the reactions of interest relies primarily upon the differences in equilibrium constants for the dominant processes. In the case of the GeI_4-Ge system we need to include the reaction

(5) $I_2 = 2I$

with reaction (1) and (2) in order to describe the system appropriately. Calculations of their respective equilibrium constants versus temperature is given in Figure 2. Note the dominance of reaction (1) in terms of magnitude of the equilibrium constant and the large temperature dependence of the reaction. A simple calculation of the species concentration at various temperature when an ampoule of 47 cm^3 volume is initially filled with 0.19 grams GeI_4 + excess germanium is shown in Figure 2. Note that the total pressure in the tube should be predominantly t GeI_2 above 500°C. These predicted values were calculated using Lever's[10] thermodynamic values. One objective of this experimental work is to confirm or provide alternative values for these thermodynamic values for the Ge-I system.

EXPERIMENTAL CONSIDERATIONS

The principal components required for obtaining Raman signature of the vapor transport gas are shown in Figure 4. The physical arrangement of the components can be seen in Figure 5. The laser Raman excitation at 488.0 or 514.5 nanometer wavelength is provided by an Argon Ion laser. Typically, 1 watt of power is used in these experiments. The 0.5 milliwatt helium neon laser is used for aligning the sample tube with the monochromator and optical train. The typical chemical vapor transport gradient to be established is across the length of the tube. In order to satisfy that requirement a three zone furnace with each zone being independently monitored and heated through proportional controllers was fabricated as seen in Figure 6. The internal structure was fabricated with a high temperature fiber material with the heating elements already enclosed, which was purchased from Aten Industries. Thus, the three zone furnace was constructed from a set of three of these assemblies, cemented together with a high temperature binder.

Since this phase of the study required an isothermal environment, a housing constructed of stainless steel with a single aperture for the laser beam to enter and the Raman signal to leave was utilized in order to eliminate thermal gradients. Thermocouples located at various points inside the housing enabled us to determine the temperature at those locations. Small adjustments in the heating controls could then linearize the thermal

characteristics of the sample tube. These features are shown in Figure 7.

The optical train uses beam steering components to direct the beam into the sample tube. The backscatter optics then collect the Raman scattered light from the sample tube and transmit it to the monochromator slit, as shown in Figure 8. The image focused onto the monochromator slit is fairly closely matched to the optical system in the spectrograph. Both spherical and cylindrical optics have been used for focussing the laser excitation beam into the sample tube. The cylindrical lens has an advantage in that the Raman scattered image matched the slit better than the point source of the spherical lens, and made alignment simpler.

The monochromator used in this work was a Spex 14018 double monochromator with 1800 lines/mm gratings. The Raman signal was detected with a RCA C31034 photomultiplier tube cooled to -140°C. Photon counting electronics were used to measure the Raman signals. Both a Spex model DPC-2 and a Princeton Applied Research model 1110 photon counter were used for the data shown in this report. Typically the dark count was less than 100 counts/sec.

EXPERIMENTAL RESULTS

Examples of spectra obtained with this system are given in Figure 9 and 10 for iodine vapor. The spectra have been obtained both in ampoules containing only iodine and in the ampoules containing GeI_4 with excess germanium. The temperature determinations inside the ampoule should be readily done with I_2 vapor. Unfortunately we did not obtain success with the anti-Stokes/Stokes ratio when we used the peak height approach with 488.0 n.m. excitation. Excitation with the 514.5 n.m. line causes fluorescence and is not reliable in our application. Later experiments with the GeI_4 tubes were not much better, since the I_2 concentration was only large enough for fluorescence to be detected. This was expected from the calculated concentration profiles in Figure 3. The spectra shown in Figure 9 is fluorescence spectra from an iodine ampoule and is a very large signal. Correspondingly Figure 10 shows the profiles obtained for Resonance Raman Scattering with the 488.0 n.m. excitation. An excellent discussion of the differences in these spectra is given by Bernstein[16]; however, these differences are not really pertinent to our results.

Spectra of GeI_4 which have been correlated with the reported data of Stammreich, H.[17] are given in Figures 11 and 12 for the Stokes and the anti-Stokes, respectively. These were obtained with the 488.0 n.m. line and are rather weak. Similar spectra obtained with the 514.5 n.m. line, as shown in Figure 13, has

fluorescence bands of I_2 as well as GeI_4. None of the spectra obtained with the GeI_4 plus excess germanium tube showed any peaks with frequency shifts in the region of 115 cm^{-1} as reported in our previous work.[17] Figure 14 shows the band observed from solid GeI_2 using 488.0 n.m. radiation in the original work with the transparent furnace.

The representative spectra shown in the preceding figures were fairly consistent in the temperature range from 250-600°C. The most prominent feature obtained from Raman scattering signals was the band around 150 cm^{-1} from the excitation line. We obtained this band using both the 488.0 and the 514.5 nanometer excitation wavelengths. This band has been assigned as the totally symmetric stretching fundamental for GeI_4 and is shifted slightly from the 160 cm^{-1} reported by Stammreich.[17] There is also observed a small temperature shift associated with the band maximum as indicated in Table 1. This small shift is peak maximum with the temperature implies that GeI_4 provides the Raman signal around 150 cm^{-1} for complete temperature range from 250-600°C. Except for the band observed at 213 cm^{-1}, which is assigned to I_2[16], no bands which can definitely be assigned to GeI_2 were observed.

In addition to the molecular identification applications of Raman scattering, temperature measurements of the vapor inside the ampoule were made using the anti-Stokes/Stokes ratio technique.

Both the I_2 band at 213 cm^{-1} and the GeI_4 band at 150 cm^{-1} were used for the temperature measurements using equation (4), but only the data with 488.0 n.m. excitation proved to be reliable. Table 1 lists some of these observations which were measured by band integration techniques. For the bands which lie fairly close to the excitation peak, the peak height measurements did not satisfy equation (4) consistently; so we then used integration of the band profile exclusively. The only disadvantage encountered is the long integration times required for measurable lineshapes.

The data in Table 1 also demonstrates the temperature resolution obtainable with this system. The use of long integration times (5-20 seconds per point) will allow about $\pm$ 5 degrees resolution. This is probably the best we can be assured of maintaining in the backscatter mode of operation.

DISCUSSION

The results obtained with these experimental conditions does allow us to determine temperature profiles and species identification in isothermal ampoule experiments. These results can be extrapolated to include quantitative measurements of concentration, if calibrations have been properly assessed, and also to include vapor transport experiments themselves. Due to the as yet unconfirmed GeI_4 to GeI_2 spectral shift as expected by our calculations, we cannot define the equilibria of the Ge-I system sufficiently to determine why the Raman spectra of GeI_2 did not occur.

The only experimental disadvantage to the Raman scattering technique is that the Raman signals can be extremely weak and using the backscatter mode of operation can be difficult if the system is not properly aligned. The chief advantage to using the backscatter mode is that the vapor absorption of the Raman signal is reduced. Since I_2, GeI_4, and GeI_2 all absorb in the 500 n.m. region, this was considered necessary for our initial experiments. If the vapor media is not absorbing in the visible then the perpendicular scatter mode is to be preferred.

The experimental technique has progressed sufficiently so that we know the furnace works properly and the Raman signals are available for temperature and concentration measurements.

Certain laser environmental controls such as constant voltage levels and uniform water flow are also being incorporated for consistent excitation intensities. In the events to follow this work we intend to work with one of Weidemeiers' ampoules from the Apollo-Soyuz flight; which has a stoichiometry that has transported and allow us to determine if the Raman bands are different from our first observations. The identification of GeI_2 in these experiments and confirmation of Lever's work still remains an objective of this work.

References

1. El Kaldis, "Principles of the Vapor Growth of Single Crystals", from Crystal Growth, Theory and Techniques, vol. 1, edited by C.H.L. Goodman, Plenum Press, 1974, London

2. Wiedemeier, H., etal, "Crystal Growth by Vapor Transport: Mechanism and Morphology of GeTe," J. Crystal Growth 13, (1972) 393

3. Wiedemeier, H., etal, "Crystal Growth and Transport Rates of GeSe and GeTe in Micro-Gravity Environment," J. Crystal Growth 31, (1975) 36

4. Wiedemeier, H., etal, "Morphology and Transport Rates of Mixed Iv-VI Compounds in Micro-Gravity," J. Electrochem. Soc. 124, (1977) 1095

5. Schafer, H., Chemical Transport Reactions, Academic Press, 1964, New York

6. Lever, R.F., "Multiple Reactions in the Vapor Transport of Solids," J. Chem. Physics, 37, (1962) 1078

7. Mandel, G., "Multiple Reactions and the Vapor Transport of Solids," J. Chem. Physics, 37, (1962) 1177

8. Faktor, M.M., etal, "Diffusional Limitations in Gas Phase Growth of Crystals," J. Crystal Growth 9, (1971) 3

9. Rolston, R.F., Iodide Metals and Metal Iodides, J. Wiley and Sons, 1961, New York

10. Lever, R.F., "Gaseous Equilibria in the Germanium Iodine System," J. Electrochem. Soc., 110, (1963) 775

11. Ross, S.D., Inorganic Infra-red and Raman Spectra, McGraw-Hill Book Co., London, 1972

12. Anderson, A., editor, The Raman Effect, Marcel Dekker, New York, 1973

13. Hendra, P.J., "Laser Raman Spectroscopy" in Vibrational Spectroscopy, vol. 3, edit., J.R. Durig, Marcel Dekker, New York, 1975

14. Smith, J.E. and Sedgewick, T.O., "Measurements of Gas Temperature Gradients Using Raman Scattering Spectroscopy", Letters in Heat and Mass Transfer, 2, (1975) 329

15. Smith, J.E. and Sedgewick, T.O., "Raman Scattering Spectroscopy Applied to the Study of Chemical Vapor Deposition Systems," J. Electrochem. Soc. 123, (1976) 254

16. Bernstein, H.J., "Resonance Raman Spectra," in Advances in Raman Spectroscopy, edited by J.P. Mathieu, Heyden and Son, Ltd., New York, 1973, p. 305

17. Stammreich, H., etal, "Raman Spectra and Force Constants of GeI_4 and SnI_4," J. Chem. Phys. 25, (1956) 1278

ACKNOWLEDGEMENTS

I wish to acknowledge the work of Mike Perry and Mike Lenox from Athens State College for various phases of this work and Jim Zwiener and Dr. Mirt Davidson of Marshall Space Flight Center for their assistance in this work. I also wish to thank Mrs. Pat Craig for typing this report.

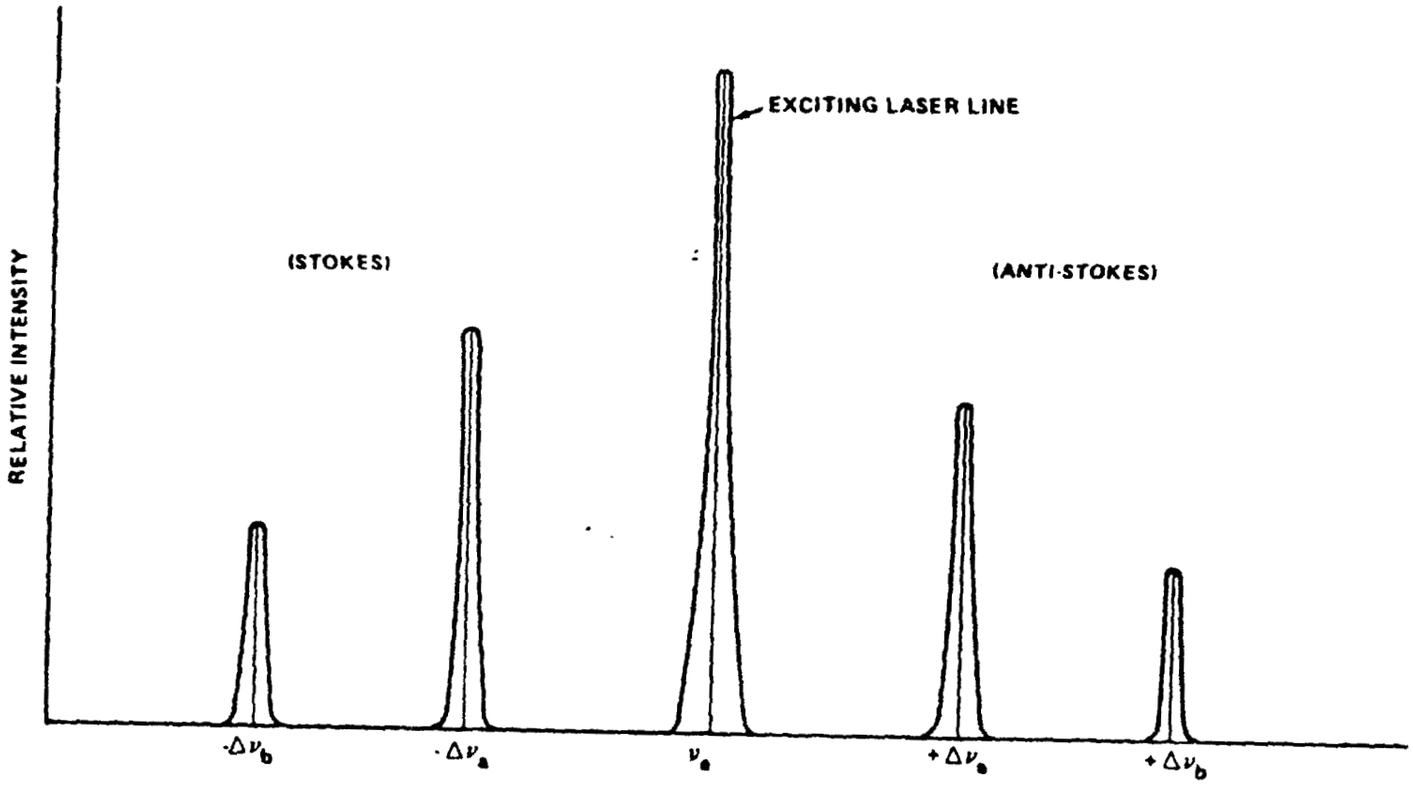

Figure 1: IDEALIZED RAMAN VIBRATIONAL SPECTRUM OF GAS MIXTURE WITH COMPONENTS "a" AND "b".

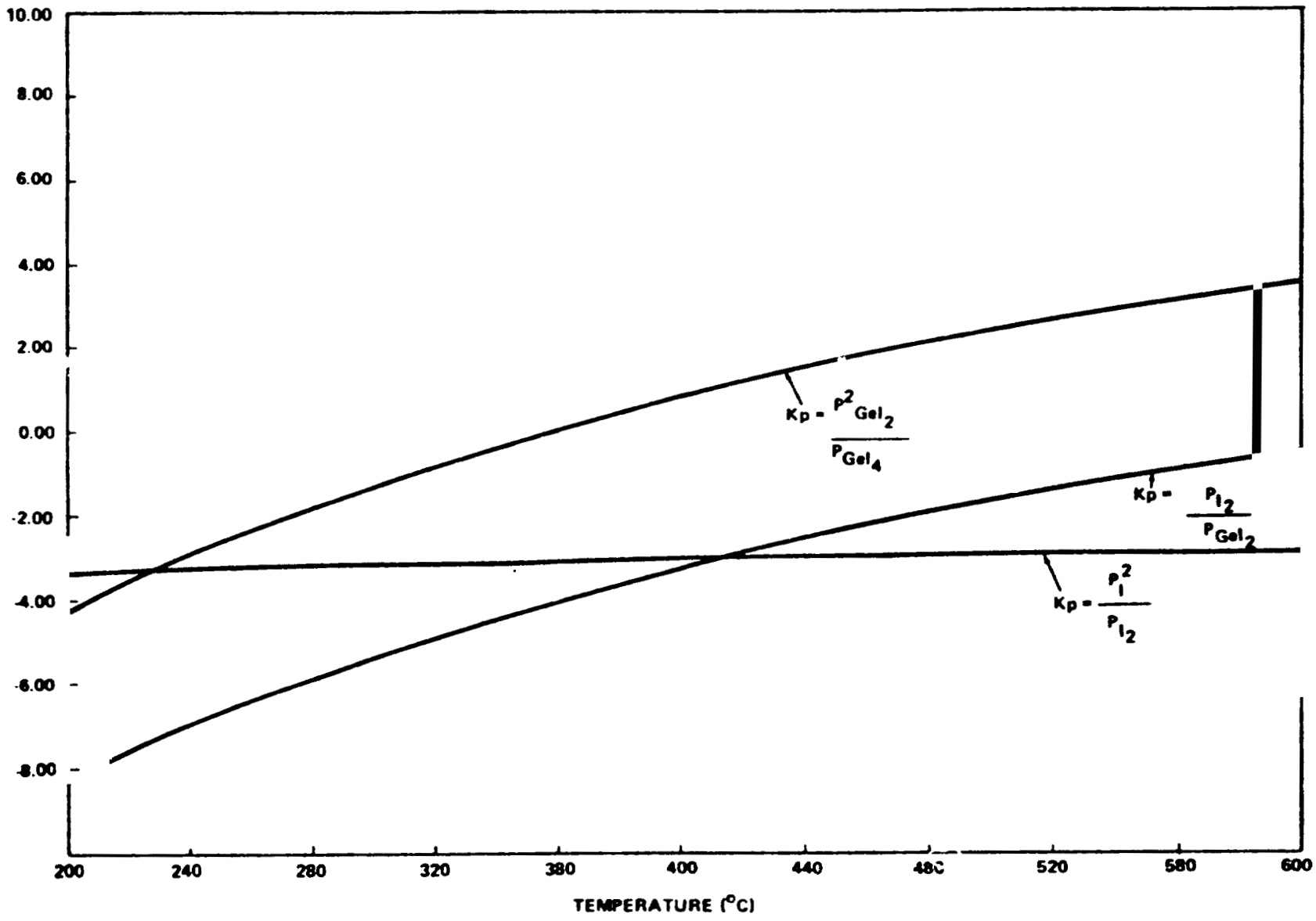

Figure 2: TEMPERATURE VARIATION OF Kp FOR THE THREE DOMINANT REACTIONS IN Ge-I SYSTEM

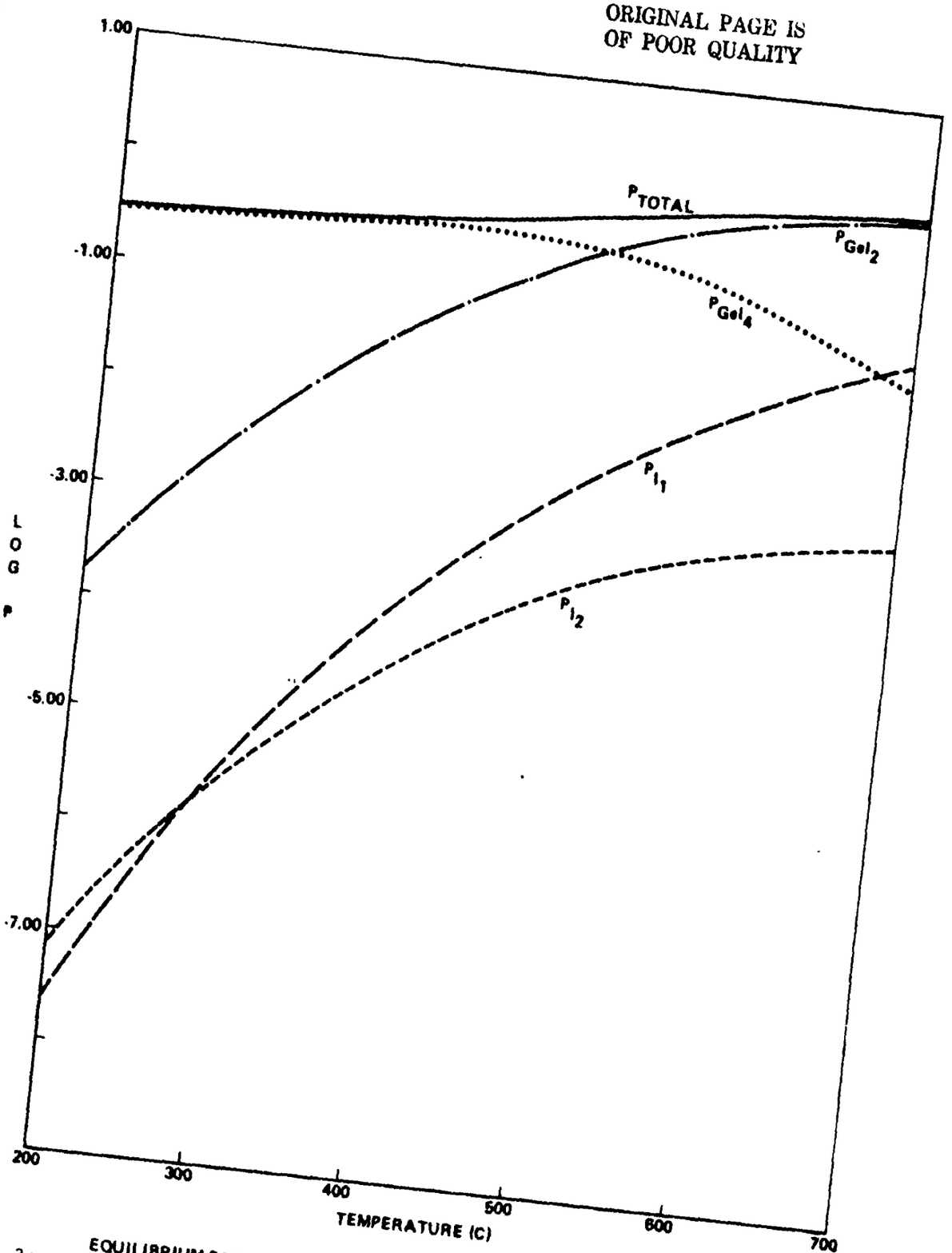

Figure 3: EQUILIBRIUM PARTIAL PRESSURES OF Ge-I SPECIES IN GeI_4 + Ge AMPOULE (0.19 GMS Ge + EXCESS GMS GeI) USING LEVER'S VALUES FOR Kp1.

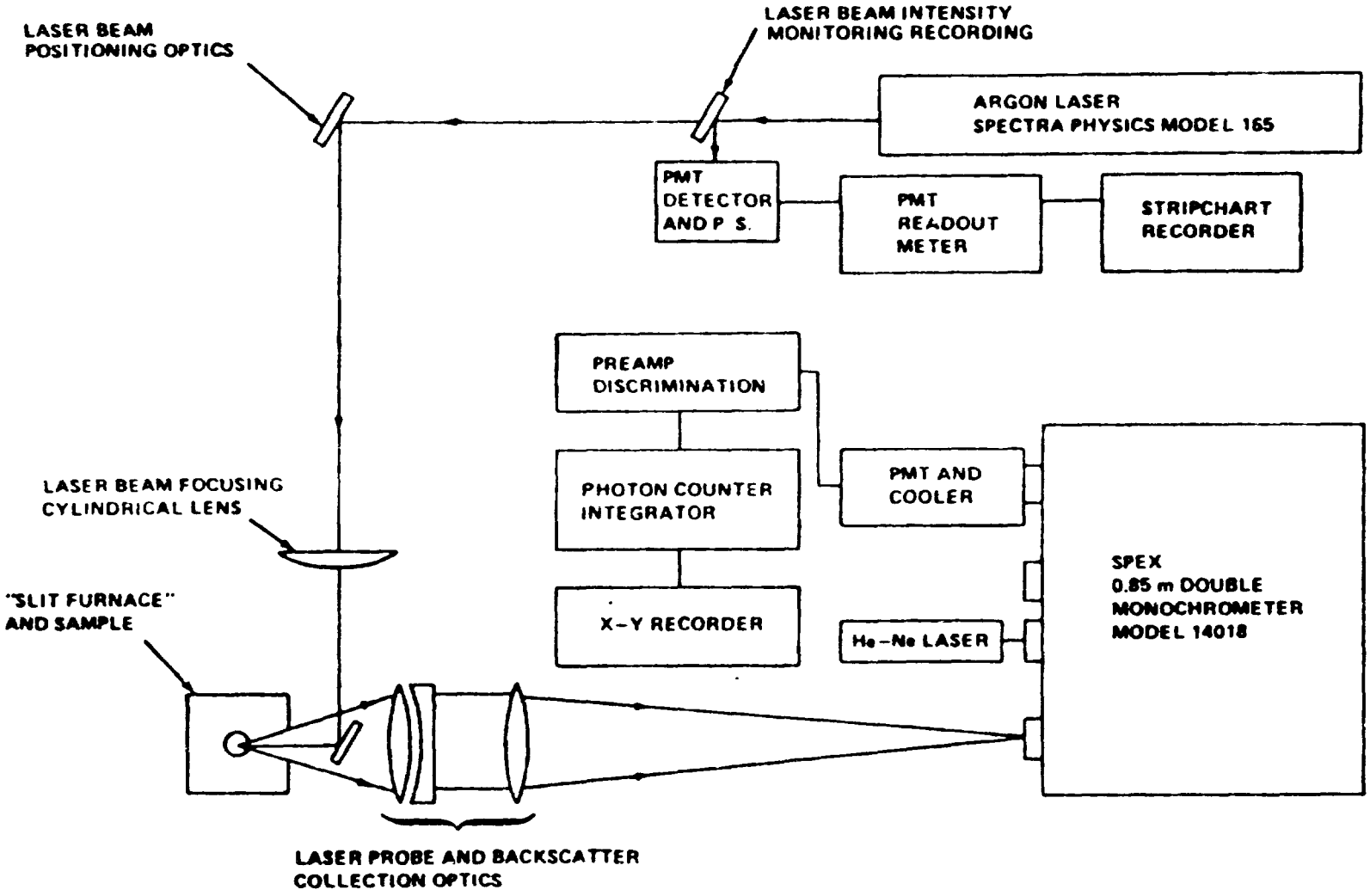

Figure 4: SCHEMATIC OF CVT RAMAN PROBE APPARATUS

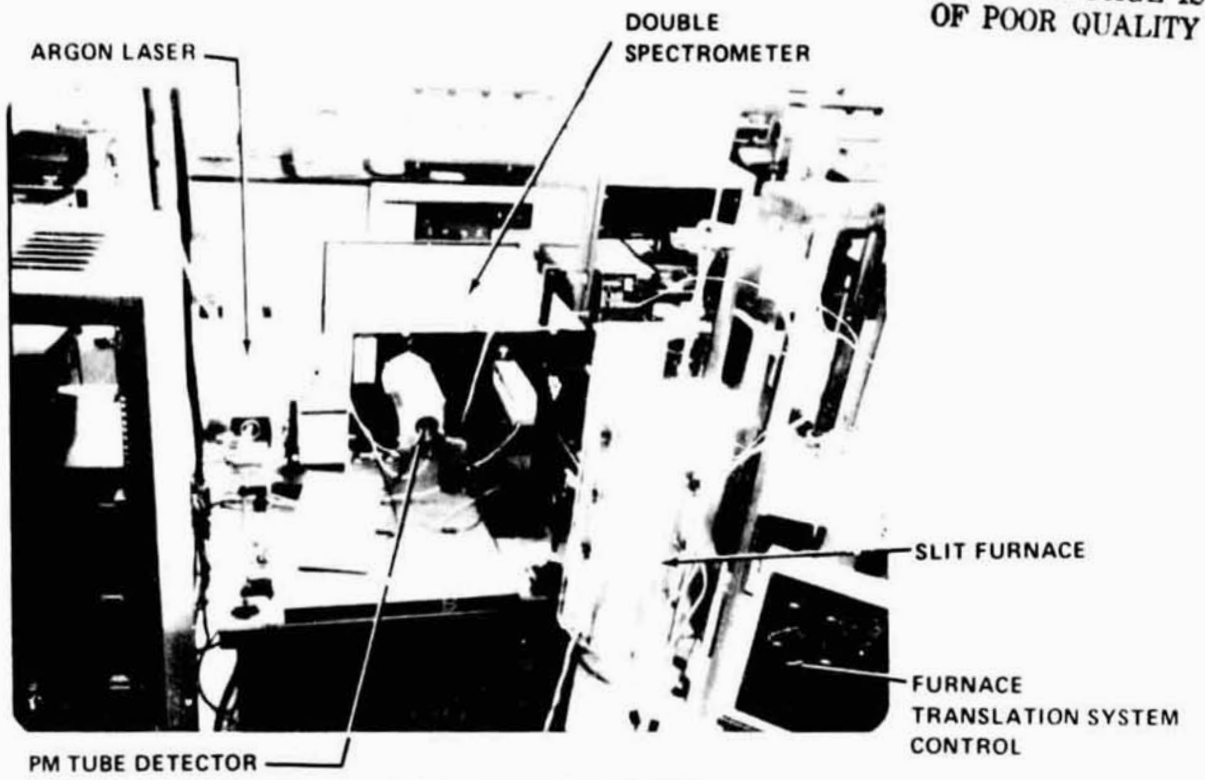

CVT RAMAN PROBE APPARATUS

PHOTO OF MAJOR COMPONENTS

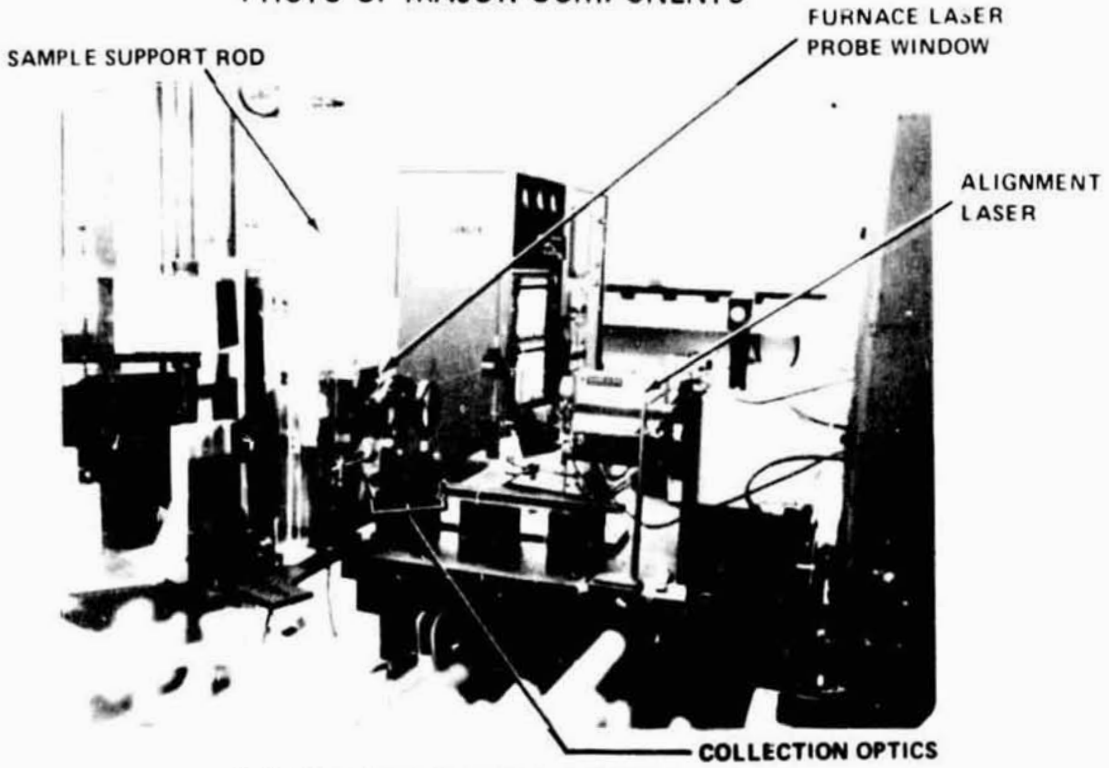

CVT RAMAN PROBE APPARATUS

PHOTO OF OPTICAL COMPONENTS

Figure 5:

ORIGINAL PAGE IS
OF POOR QUALITY

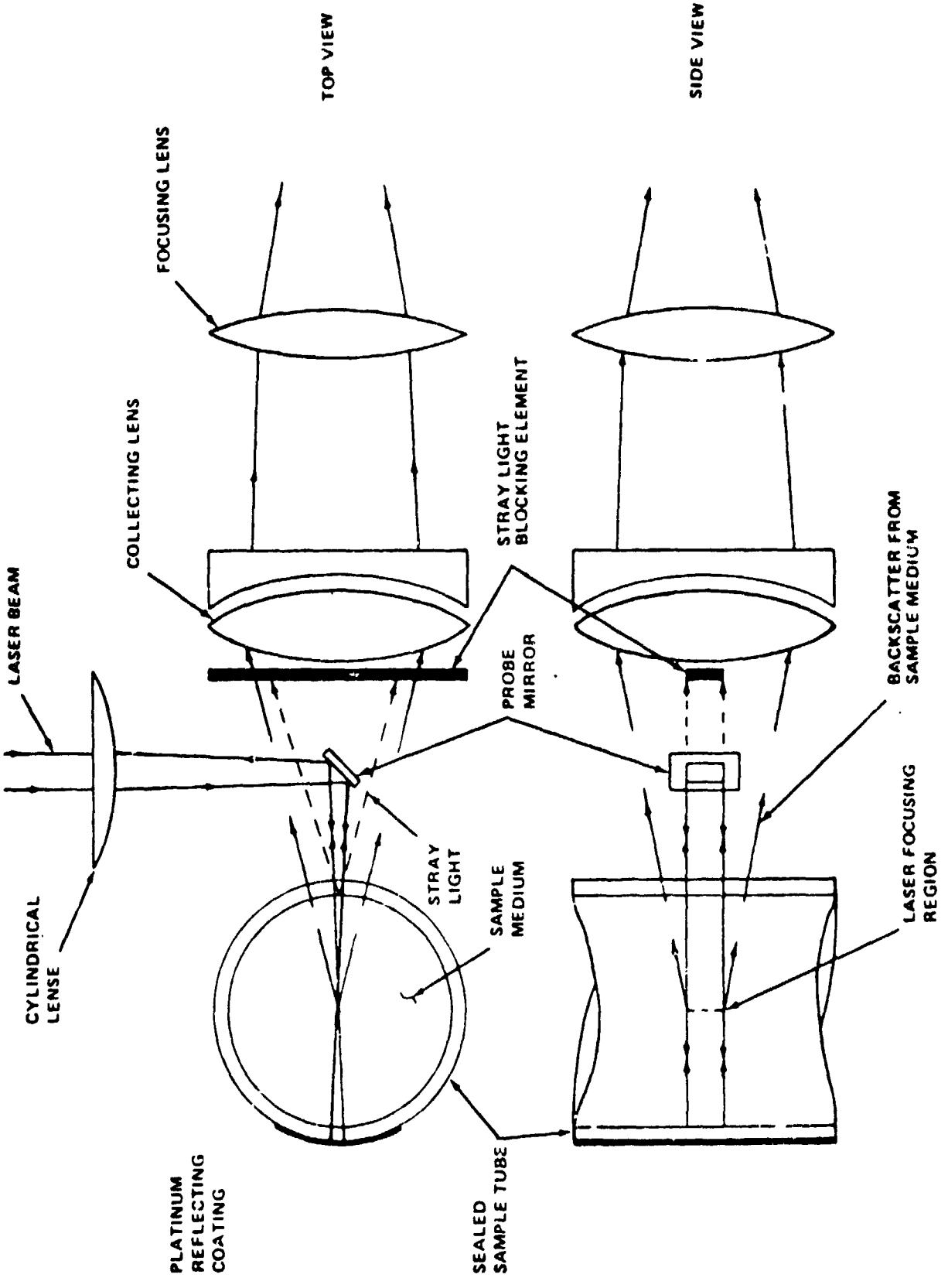

Figure 6: SCHEMATIC OF LASER PROBE AND BACKSCATTER COLLECTION OPTICS

Figure 7:

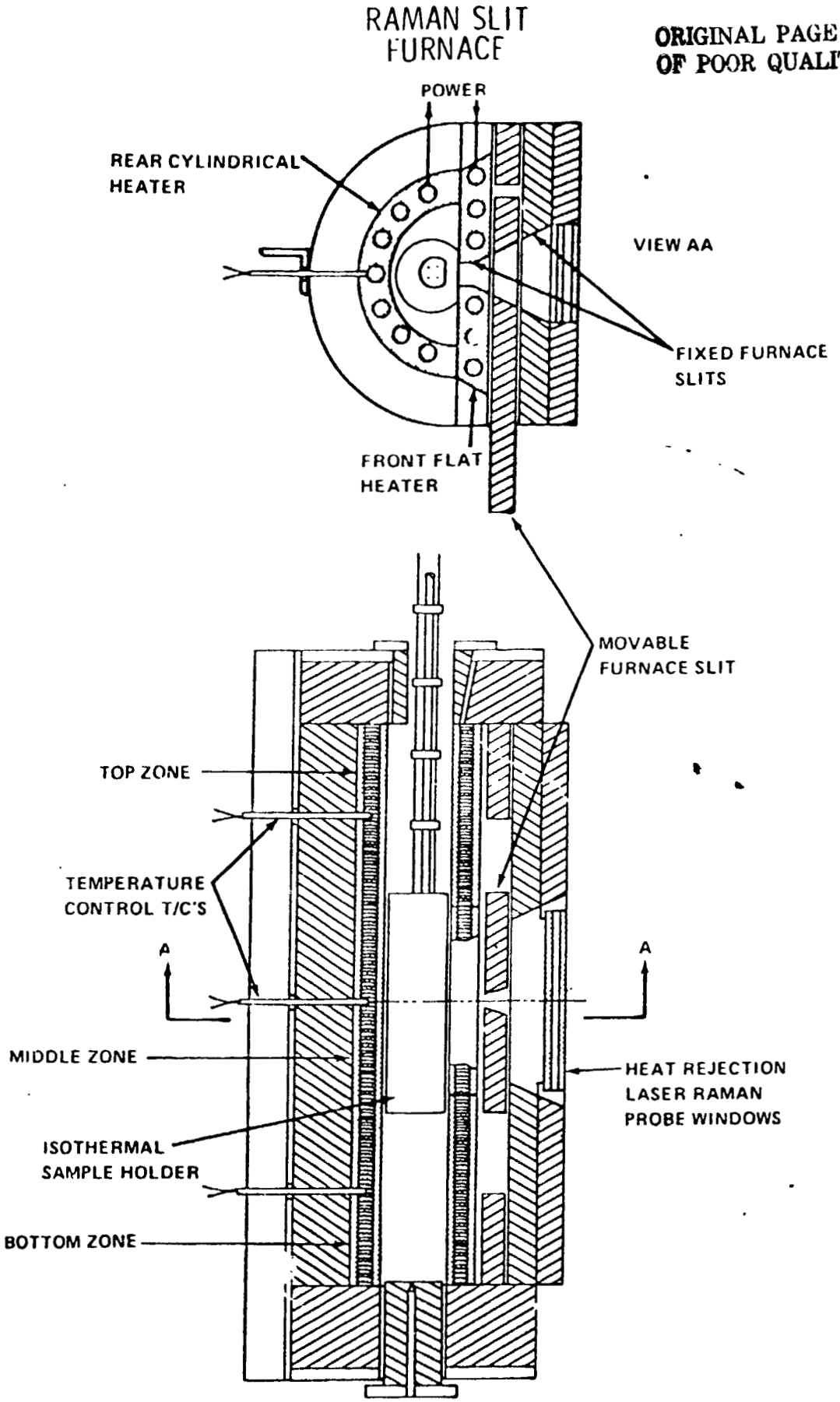
RAMAN SLIT FURNACE
ORIGINAL PAGE IS OF POOR QUALITY
POWER
REAR CYLINDRICAL HEATER
VIEW AA
FIXED FURNACE SLITS
FRONT FLAT HEATER
MOVABLE FURNACE SLIT
TOP ZONE
TEMPERATURE CONTROL T/C'S
A
A
MIDDLE ZONE
HEAT REJECTION LASER RAMAN PROBE WINDOWS
ISOTHERMAL SAMPLE HOLDER
BOTTOM ZONE

Figure 8: ISOTHERMAL SAMPLE HOLDER

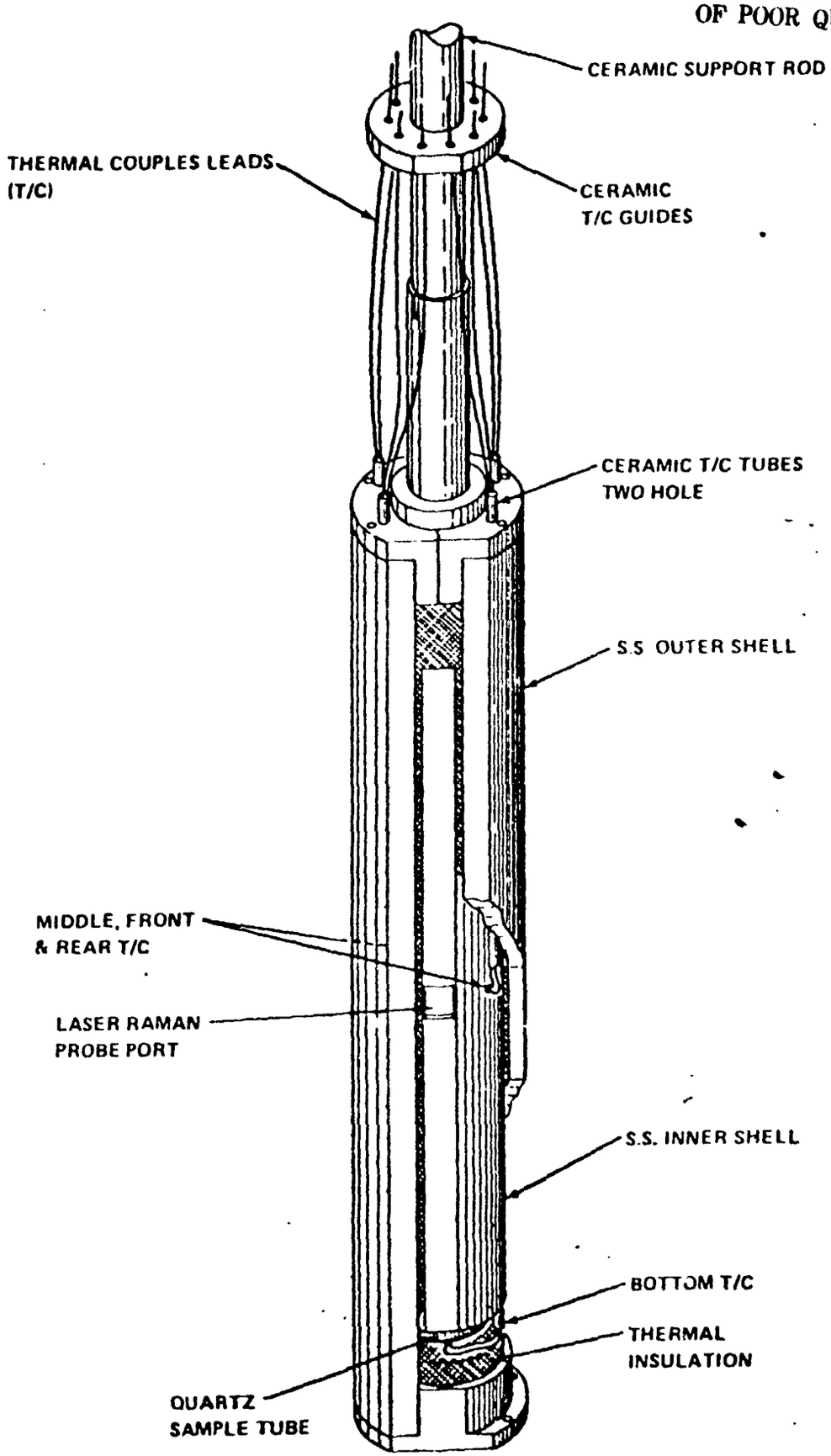

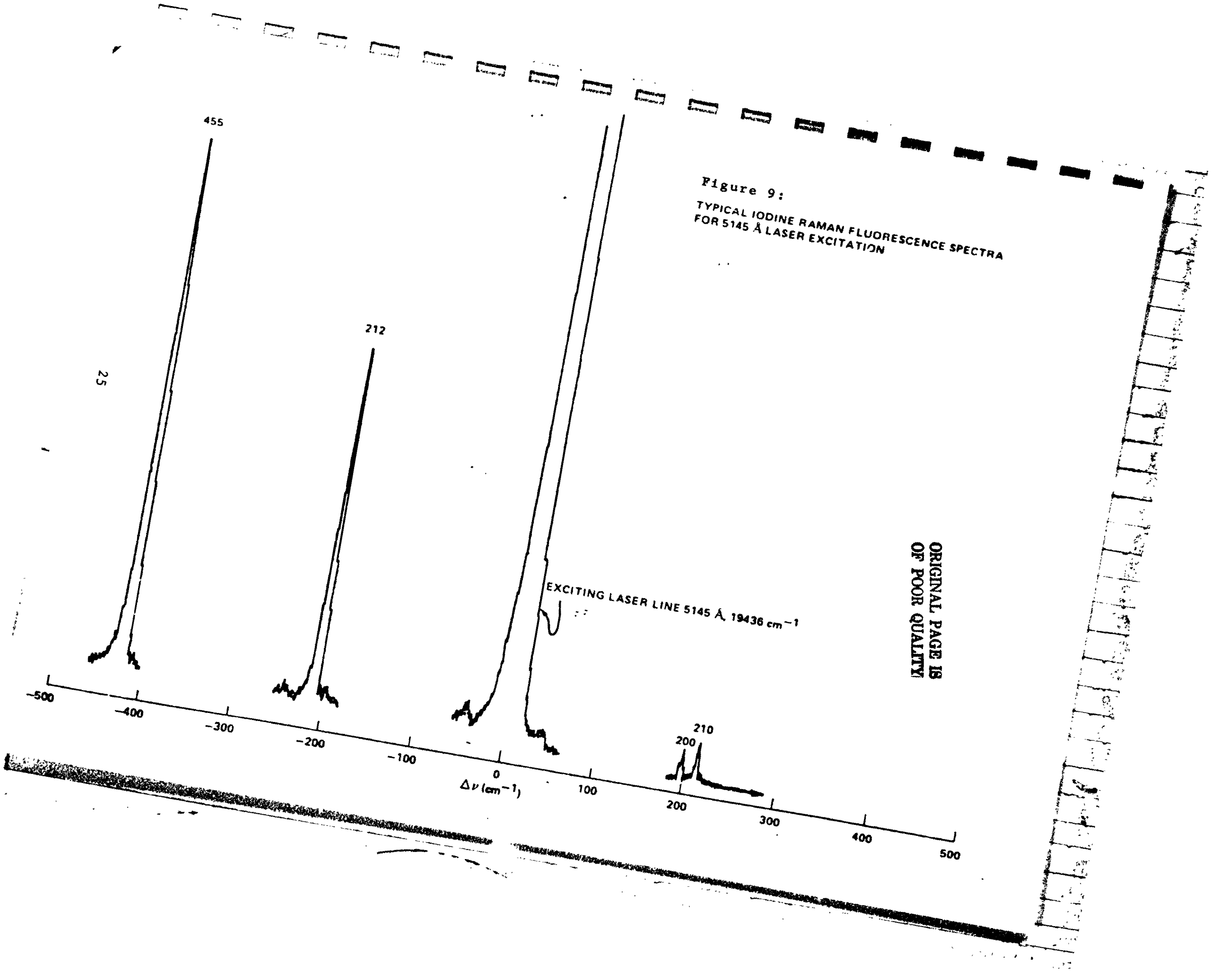

Figure 9:

TYPICAL IODINE RAMAN FLUORESCENCE SPECTRA FOR 5145 Å LASER EXCITATION

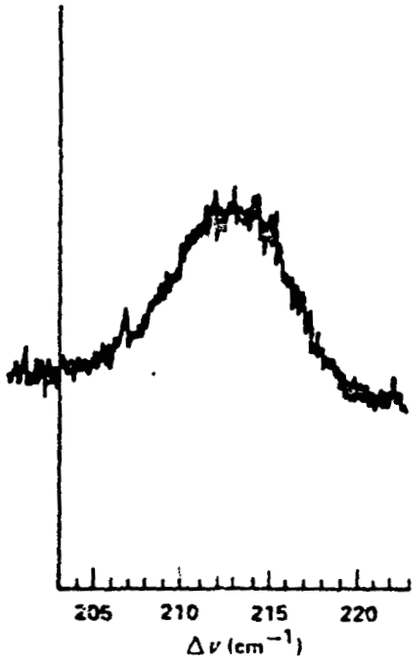

ANTISTOKES RAMAN BAND FOR IODINE VAPOR
USING 4880 Å LASER EXCITATION

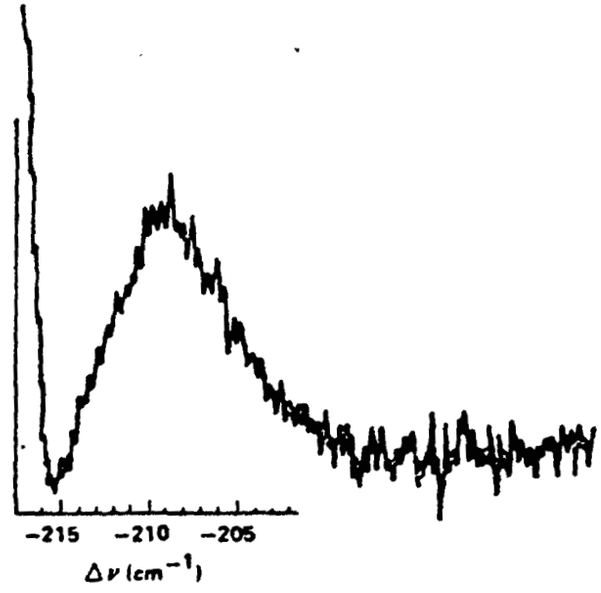

STOKES RAMAN BAND FOR IODINE VAPOR
USING 4880 Å LASER EXCITATION

Figure 10: Spectra showing types of bands observed for iodine with resonance Raman scattering

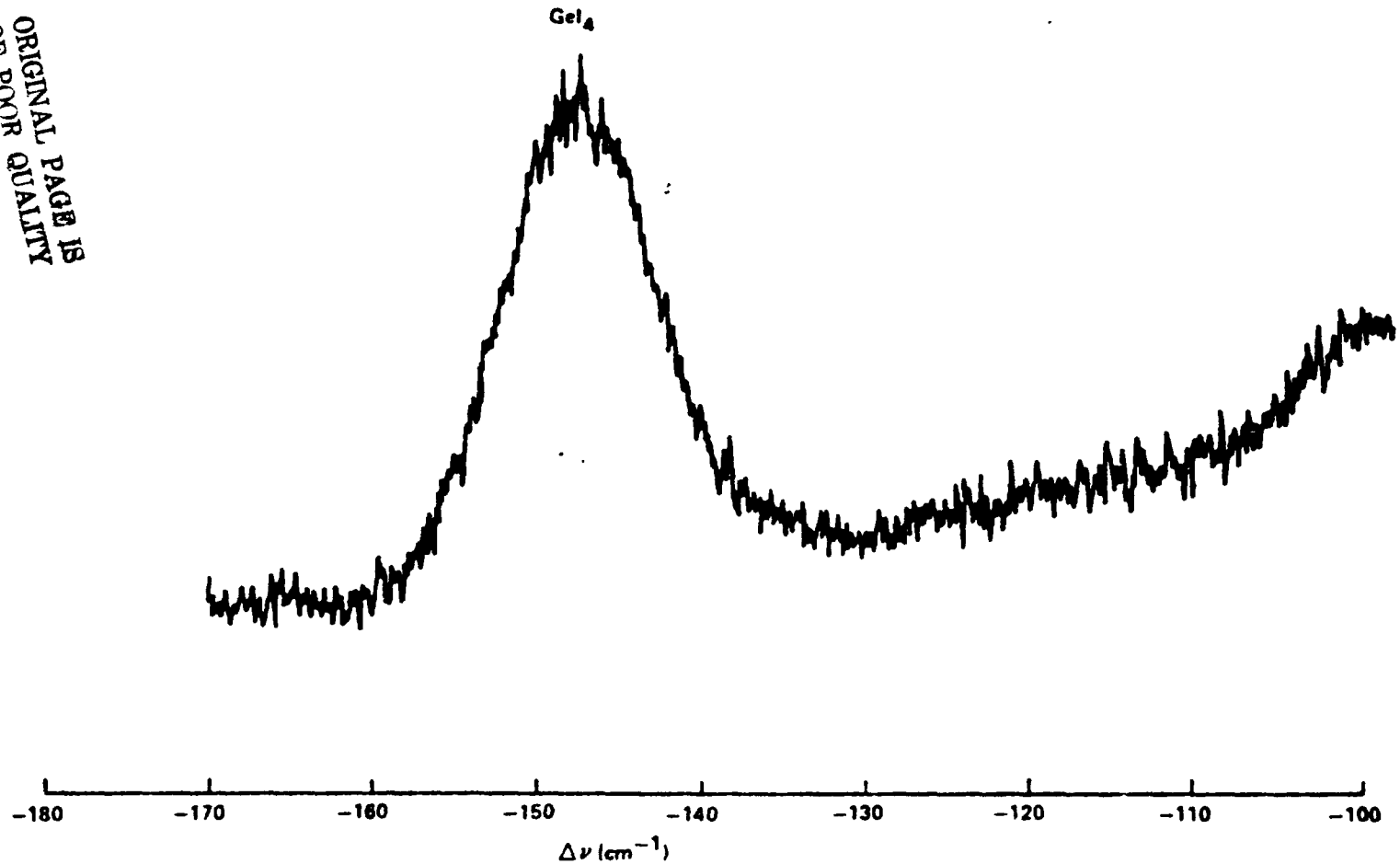

Figure 11: STOKES RAMAN BAND FOR GeI_4 VAPOR USING 4880 Å LASER EXCITATION

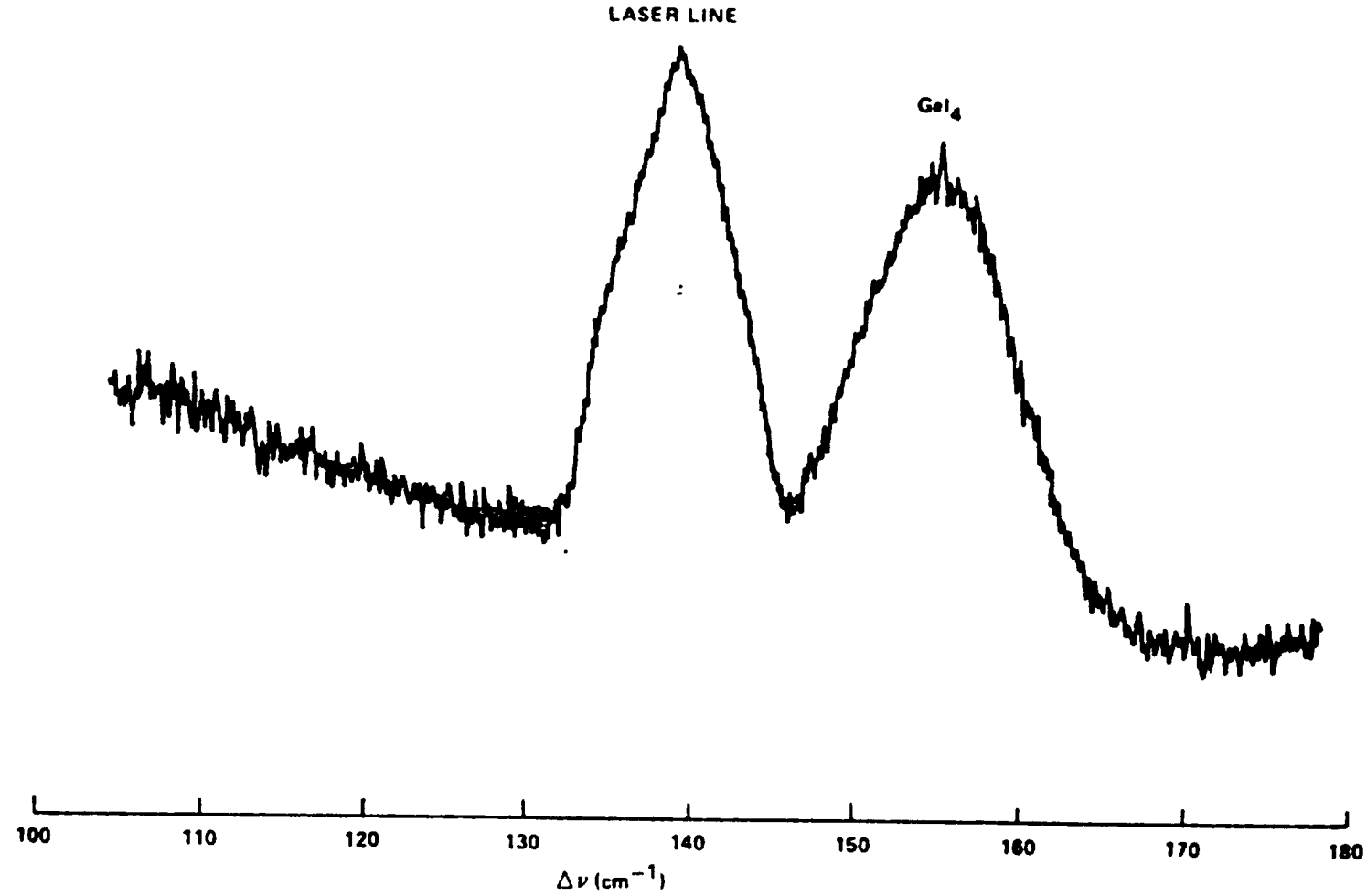

Figure 12: ANTISTOKES RAMAN BAND FOR GeI_4 VAPOR USING 4880 Å LASER EXCITATION

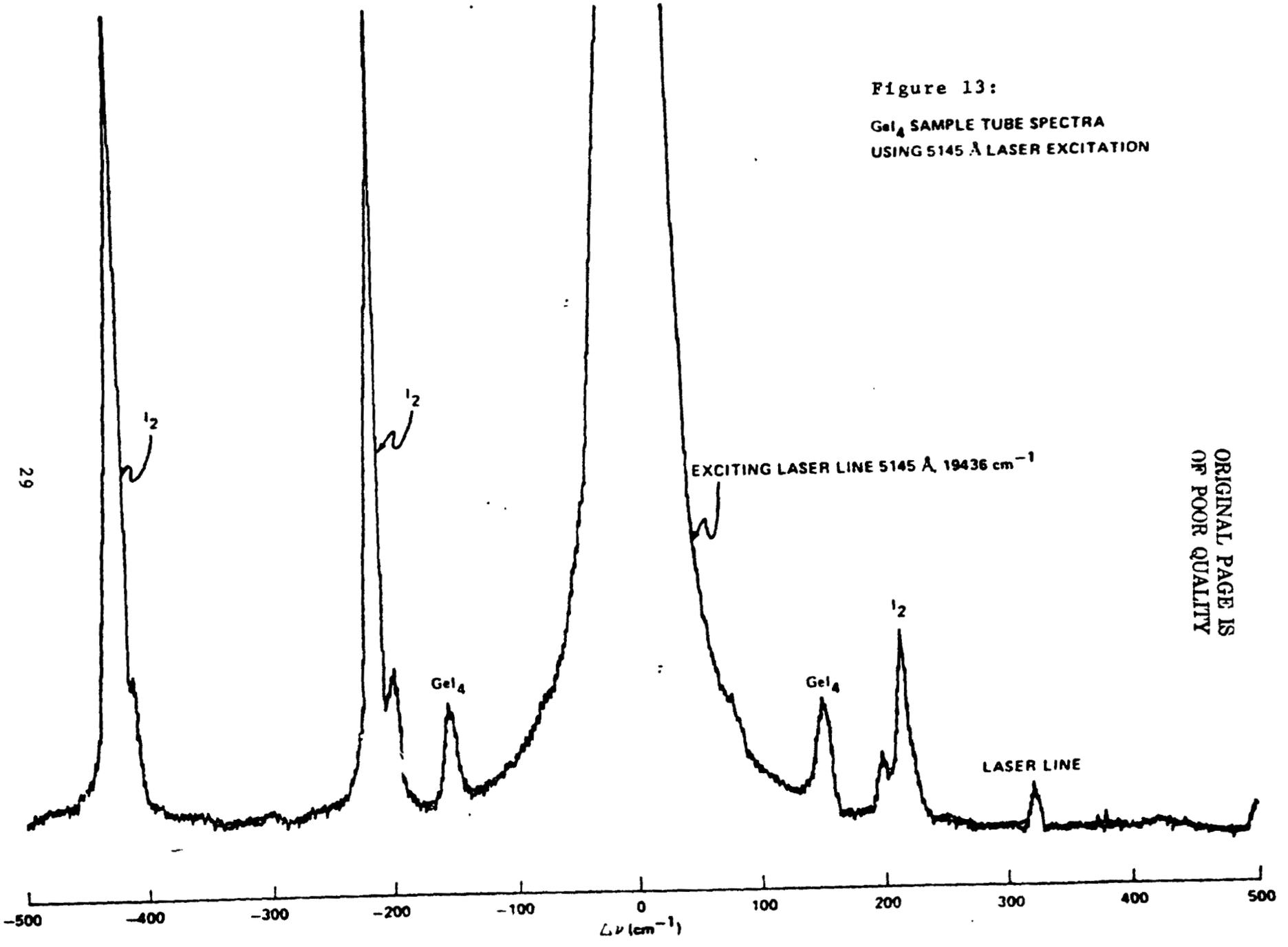

Figure 13:

GeI_4 SAMPLE TUBE SPECTRA
USING 5145 Å LASER EXCITATION

ORIGINAL PAGE IS
OF POOR QUALITY

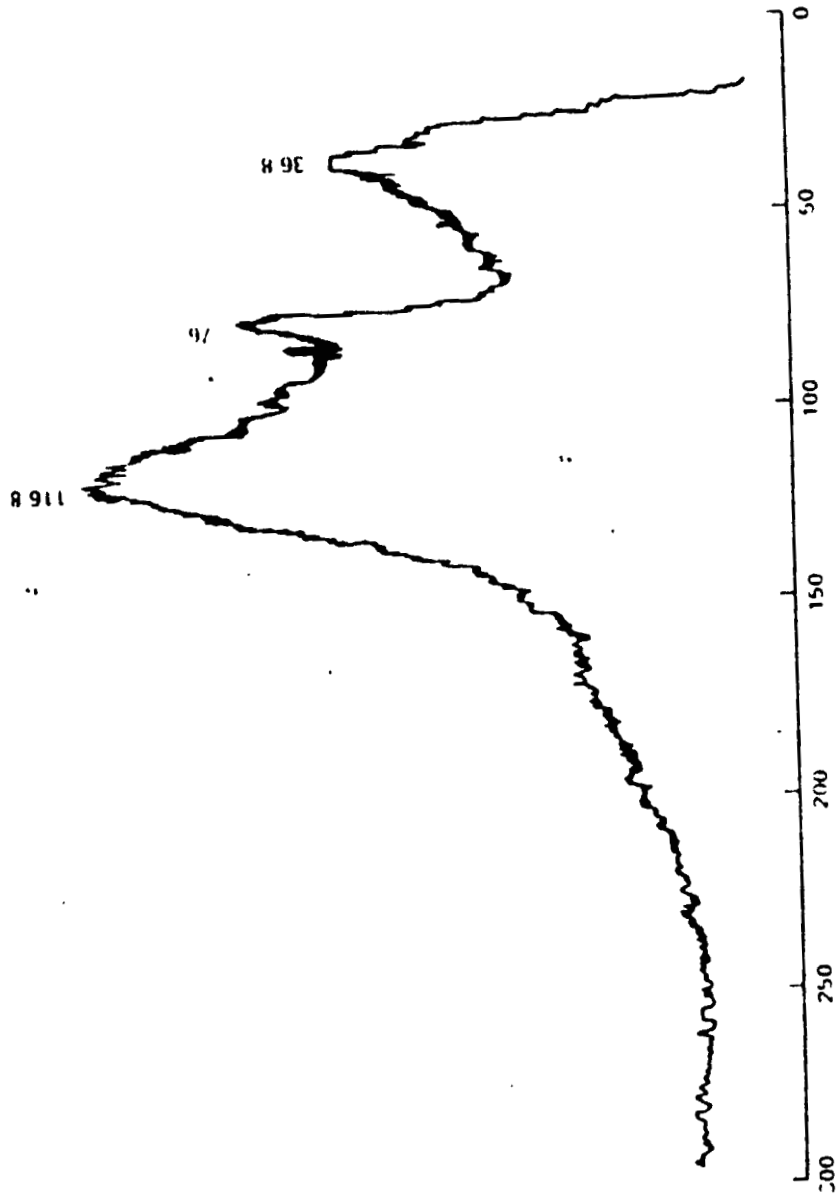

Figure 14: RAMAN BANDS FOR SOLID GeI_2 AT ROOM TEMPERATURE

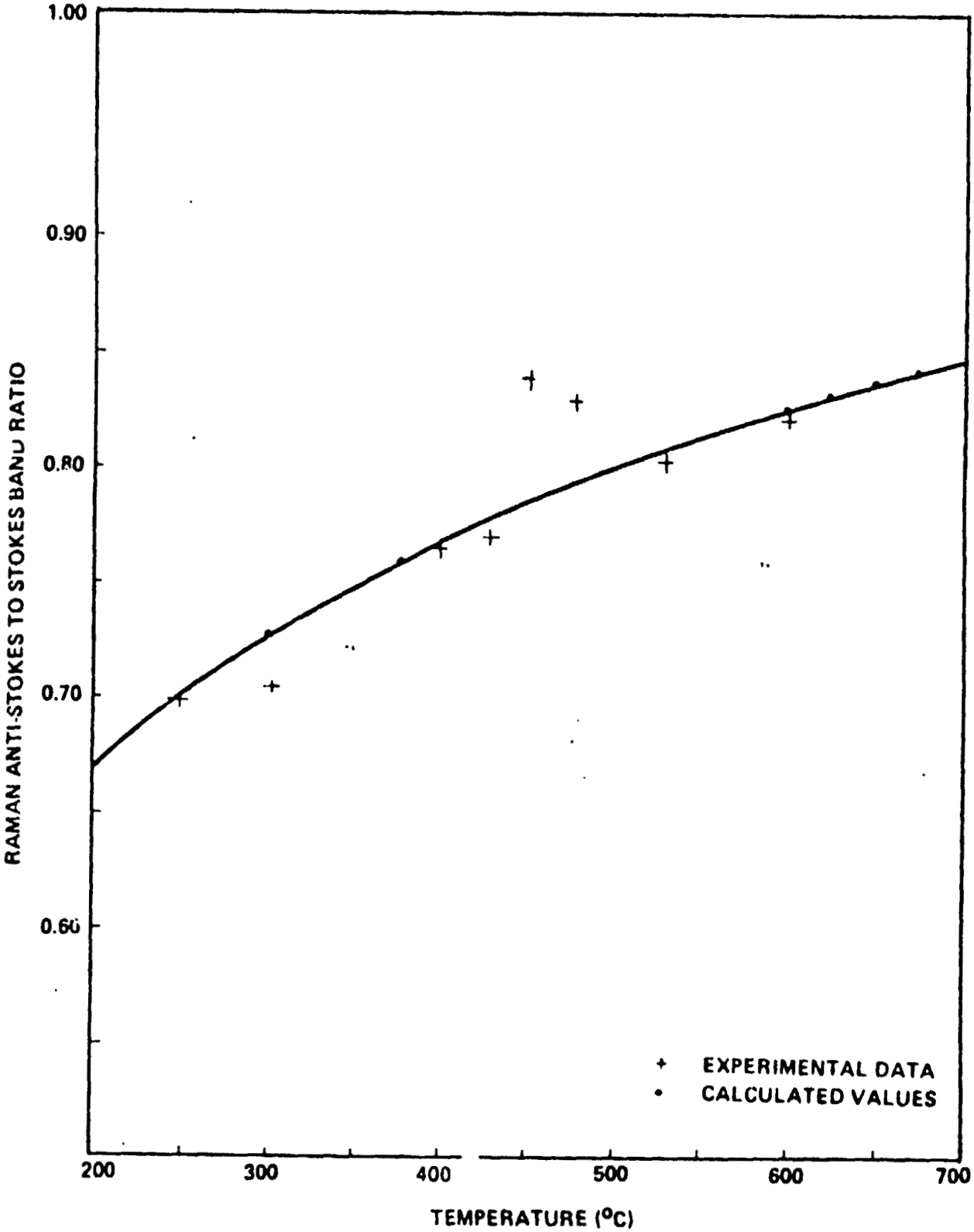

Figure 15: TEMPERATURE MEASUREMENTS OF Ge-I SYSTEM USING ANTI-STOKES/STOKES RATIO FOR RAMAN BAND AT 150 cm^{-1}, LASER EXCITATION USING THE 488.0 nm LINE.

Table 1. SUMMARY OF EXPERIMENTAL DATA FROM LASER RAMAN SCATTERING FOR TEMPERATURE MEASUREMENT IN Ge-I SYSTEM

RUN NUMBER	TEMPERATURE CENTRIGRADE	RAMAN SHIFT CM-1	EXCITATION WAVELENGTH NM	CALCULATED A/S RATIO	MEASURED A/S RATIO (T)	REMARKS
417	253 0	153.7	488 0	0.703	0.693 (234)	WIDE SLITS NOISY BACKGROUND
428	426.0	152.9	488.0	0.778	0.769 (399)	LESS WIDE SLITS GOOD BACKGROUND
501	451.5	151.8	488.0	0.786	0.841 (659)	OVERLAPPING LASER LINE
502	476.0	151.5	514.5	0.797	1.269	NOISY BACKGROUND CLEAN SIGNALS
503	523.0	151.7	514.5	0.811	1.190	GOOD SIGNALS GOOD BACKGROUND
504	524.0	151.4	488.0	0.808	0.804 (507)	OVERLAPPING LASER LINE
505	304.0	153.0	488.0	0.729	0.707 (259)	NOISY SIGNAL POOR RESOLUTION
510	471.0	151.1	488.0	0.793	0.830 (609)	OVERLAPPING LASER LINE AND NOISY
515	595.0	150.4	488.0	0.826	0.821 (571)	GOOD SIGNAL GOOD BACKGROUND
606	395.0	152.7	514.5	0.770	1.360	GOOD SIGNAL GOOD BACKGROUND
607	395.0	152.2	488.0	0.767	0.763 (383)	GOOD SIGNAL GOOD BACKGROUND